SIMULATION OF NEWLY DESIGNED VORTEX GENERATORS FOR OPTIMIZING FLUID MIXING EFFICIENCY IN COMPACT STATIC MIXERS WITH SINGLE-EXIT CONFIGURATION

by

Noureddine KAID[a], Mustafa BAYRAM[b*], Jihad ASAD[c], Muhammad ATIF[d], Muataz S. ALHASSAN[e], Houari AMEUR[a], Hijaz AHMAD[f, g], and Younes MENNI[a,h]

[a] Department of Technology, University Center Salhi Ahmed Naama (Ctr. Univ. Naama), Naama, Algeria
[b] Department of Computer Engineering, Biruni University, Istanbul, Turkey
[c] Department of Physics, Faculty of Applied Science, Palestine Technical University- Kadoorie, Tulkarm, Palestine
[d] Department of Physics and Astranomy, College of Science, King Saud University, Riyadh, Saudi Arabia
[e] Division of Advanced Nano Material Technologies, Scientific Research Center, Al-Ayen University, Thi-Qar, Iraq
[f] Section of Mathematics, International Telematic University Uninettuno, Roma, Italy
[g] Operational Research Center in Healthcare, Near East University, Nicosia/Mersin, Turkey
[h] National University of Science and Technology, Dhi Qar, Iraq

Original scientific paper
https://doi.org/10.2298/TSCI2304337K

This research paper presents a highly significant study on a new type of static mixer, using advanced numerical simulations to assess its mixing efficiency. The mixer's unique T-shaped design with a spherical mixing chamber and side entrances deviates from traditional designs, resulting in smooth fluid-flow and reduced risk of blockages. The mixer employs hydrodynamic pumps to create a vortex, enhancing mixing. Numerical simulations reveal detailed insights into flow behavior and mixing performance, demonstrating an impressive 94% mixing efficiency within a 2 cm diameter sphere. The innovative design and technique offer practical solutions to industrial mixing problems, benefiting the chemical, pharmaceutical, and related industries. The high mixing efficiency leads to cost savings and improved product quality, while achieving the highest mixing index at Re = 650 sets a new milestone in static mixing. These findings contribute to applied mechanics and optimize industrial mixing processes.

Key words: *compact static mixers, spherical mixing chamber, vortex generators, hydrodynamic pumps, mixing efficiency, 3-D simulation*

Introduction

Manufacturing industries have adopted static mixers, referred to as motionless mixers. Despite this, new concepts and applications are being developed. In single-pass or recycling cylinders, statistical mixers are used to supplement or even replace conventional agitators. Since they can be used in continuous processes at a lower cost, they can provide comparable and better results than traditional agitation. Because they do not have movable parts,

* Corresponding author, e-mail: mbayram34@gmail.com

fixed mixers use less energy and require less maintenance. They provide a more controllable and evolvable dilution rate in lot-fed systems and may allow for the homogenization of nutrient fluxes within a short residence time. Static mixers were not commonly used in transformation processes until the 1970's. However, the patent dates much earlier [1]. A patent from 1874 describes a stationary mono-element gas-air mixer.

Manufacturers of static mixers provide various mixing processes, including laminar and turbulent ones. The laminar flux mixture is founded on flux fractionation and recombination. In the case of turbulence, the components produce more turbulence than the identical flat tube. Mixtures have been employed in processes requiring mixing, reaction, dispersion, heat transmission, and mass transfer. Hobbs and Muzzio [2] investigated Kenic's static mixer and analyzed it digitally using Lagrangian methods. In a related study, Yoo *et al.* [3] explored the effectiveness of passive mixing methods and introduced the HVW micro-mixer, which combines vertical and horizontal flows to enhance mixing efficiency. The turbulent flow model and the mixing characteristics of a high-performance vortex mixer (HEV TM) have been studied using numerical fluid dynamics simulations [4]. In their research, Kim *et al.* [5] investigated a novel micromixer that employs a quasi-active rotor designed specifically for micro-installation applications. In their study, Viktorov *et al.* [6] explored a new passive micromixer design based on the split and recombine (SAR) principle. Yang *et al.* [7] introduce a novel micromixer, which is a reactor that utilizes spatially distributed micro-jet networks to enhance mixing efficiency. A 3-D helical microchannel was assembled with a double 'C' form to enhance the fluid mixture negatively by adopting anarchic austerity features [8], with a Reynolds number ranging from 6 to 70. An SMX-type static mixer section was altered to alter mixing behavior [9]. The KM static mixers have been evaluated using laser-induced planar fluorescence for mixing non-Newtonian, Newtonian, and time-independent fluids [10]. In their study, Fradette *et al.* [11] employed a Sulzer SMX mixer to disperse gas in various types of fluids, including viscous, Newtonian, and non-Newtonian fluids. Experiments were conducted under laminar flow conditions, using a xanthan gum solution as the test fluid, as reported by Jegatheeswaran *et al.* [12]. Numerical investigations were conducted to explore the features of the combination of evaporation and charge loss in marine catalytic reduction applications. To this end, two mixers, one of which is a line mixer while the other is a swirling mixer, were suggested [13]. Zidouni *et al.* [14] employed the Euler-Euler method to simulate the solar liquid gas model in a constant-speed helicoidal mixer. A positron emission particle tracking and magnetic resonance imaging analysis of laminar mixtures were performed in an SMX static mixer [15]. Edwards *et al.* [16] studied the behavior of single-phase liquids in mechanically agitated containers. This study only provides a limited number of examples to demonstrate how static mixing units have become essential in continuous processes that prioritize economics and ecology [17]. A model was developed to predict the concentration response of a solvent extraction column with multiple mixers to changes in the inlet stream concentration [18]. Hamouda [19] demonstrates the significance of fluid mechanics, which students at higher institutions of technical education should understand. A study was conducted to compare the performance of a tubular crystallizer with gaps between Kenics-like mixing components to that of a conventional Kenics static mixer in the crystallization of lysozyme from a solution [20].

The objective of this paper is to evaluate the efficacy of a new tiny static mixer, which has been designed and built from scratch. The mixer features a *T*-shaped design with a spherical cavity, two opposing side entrances, and an exit normal to the plane of the inlet, without any internal components. Unlike previous studies, this design has not been previously explored for fluid mixing. To assess the mixer efficiency, various criteria such as pressure

drop and coefficient of variation were used to evaluate the quality of the mixture. The key element in this process is the generated vortex, which facilitates the mixer maintenance and does all the work. By studying the fluid mixing using this design, we aim to provide insights into the potential applications of this mixer in various industries, such as chemical and pharmaceuticals. Our findings can lead to the development of more efficient and cost-effective mixing technologies.

Simulation and design

The passive mixer being studied in this experiment is a 3-D sphere with a diameter of 2 cm, as shown in fig. 1. This same sphere is connected to two cylindrical entrances of 0.5 cm diameter, while the outlet is a cylindrical cylinder of 0.7075 cm in diameter oriented normally to the two cylindrical surfaces, as illustrated in fig. 2.

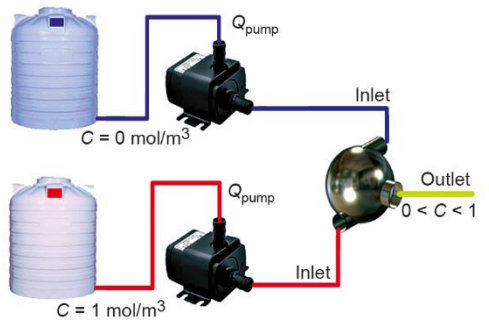

Figure 1. Mixing process

The overall 3-D model of the mixer is shown in fig. 3. The spherical shape of the mixer facilitates the generation of a vortex, which enhances the mixing of fluids. The two cylindrical entrances serve as inlet points for the fluid to enter the mixer, while the outlet enables the mixed fluid to exit the system.

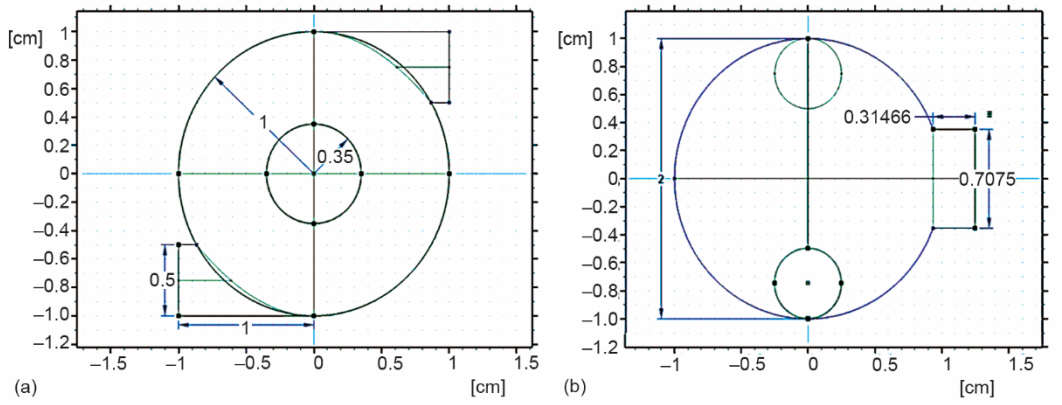

Figure 2. The *T*-Shape static mixer dimension

This simple yet effective design provides an innovative solution for various applications in chemical and pharmaceutical industries. By studying the behavior of the passive mixer and its flow characteristics, we aim to gain a deeper understanding of the mixing process and its potential applications in industry. Our findings can lead to the development of more efficient and cost-effective mixing technologies, ultimately benefiting society and the environment.

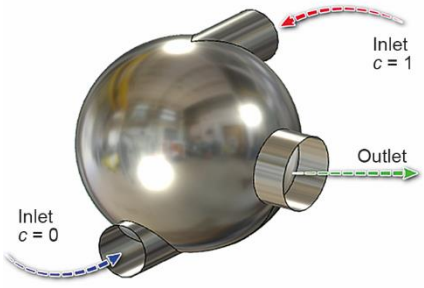

Figure 3. The 3-D view of the static mixer

In terms of boundary conditions, velocity inputs, u_{in}, were specified as the inputs, while the outlet static gauge pressure was defined as zero ($p = 0$). The wall was set as a fixed wall without sliding conditions. The simulation was conducted multiple times, with the entrance rate into the laminar flow regime being altered by varying the Reynolds number, which was set to 100, 500, 1000, 1500, 2000, and 2500. The lateral input concentrations were 0 and 1, respectively. Table 1 provides a detailed overview of the key characteristics of the mixer, as well as the relevant fluid properties and boundary conditions.

Table 1. Mixer characteristics, fluid properties and boundary conditions

Name	Expression/value	Unit	Description
ρ	998	[kgm^{-3}]	Density
μ	0.001	[Pa·s]	Dynamic viscosity
D_h	2	[cm]	Sphere diameter
$D_{h,out}$	0.7075	[cm]	Outlet diameter
$D_{h,in}$	0.5	[cm]	Inlet diameter
v_{in}	$Re\mu/D_{h,in}/\rho$	[ms^{-1}]	Inlet velocity
Re	100-2500	1	Reynolds number
L	0.31466	[cm]	Exit tube length
q_{in}	$(\rho v_{in} p_i D_{h,in})^{2/4}$	[kgs^{-1}]	Mass flow rate
G_{Qpump}	$2q_{in}$	[kgs^{-1}]	Global flow rate
R	$D_h/2$	[cm]	Tube radius
R_{in}	$D_{h,in}/2$	[cm]	Inlet tube radius
Q_{pump}	$q_{in}/\rho d_p$	[W]	Pumping power
d_p	Average inlet, p	[Pa]	Pressure loss

It should be emphasized that the following analysis assumes that the fluid-flows are miscible, laminar, and incompressible with homogenous characteristics and minimal gravity and temperature change effects in the computing area. As the literature describes, diffusion has complete control over the mixing method. The process of distributing substances from a high concentration to a low concentration via Brownian motion, which leads to the gradual mixing of the components, is known as diffusion. The Navier-Stokes and convection-diffusion equations have been utilized to solve for Newtonian and incompressible fluids. The governing equations are as follows, while disregarding the body force and gravity:

$$\nabla U = 0 \tag{1}$$

$$\rho U \nabla U = -\nabla P + \mu \nabla^2 U \tag{2}$$

$$U \nabla c = D \nabla^2 c \tag{3}$$

In cylindrical coordinates (r, θ, z) under steady-state conditions, the aforementioned equations yield the following expressions.

Continuity equations in cylindrical coordinates (*r, θ, z*):

$$\frac{1}{r}\frac{\partial}{\partial r}(rU_r)+\frac{1}{r}\frac{\partial U_\theta}{\partial \theta}+\frac{\partial U_Z}{\partial z}=0 \tag{4}$$

Momentum equation:

r – component:

$$\rho\left(U_r\frac{\partial U_r}{\partial r}+\frac{U_\theta}{r}\frac{\partial U_r}{\partial_r}-\frac{U_\theta{}^2}{r}+U_Z\frac{\partial Uz}{\partial Z}\right)=$$

$$=-\frac{\partial P}{\partial r}+\mu\left\{\frac{\partial}{\partial r}\left[\frac{1}{r}\frac{\partial}{\partial r}(rU_\theta)\right]+\frac{1}{r^2}\frac{\partial^2 U_r}{\partial \theta^2}-\frac{2}{r^2}\frac{\partial U_\theta}{\partial \theta}+\frac{\partial^2 U_r}{\partial z^2}\right\} \tag{5}$$

θ – component:

$$\rho\left(U_r\frac{\partial U_\theta}{\partial r}+\frac{U_\theta}{r}\frac{\partial U_\theta}{\partial \theta}+\frac{U_r U_\theta}{r}+U_Z\frac{\partial U_\theta}{\partial Z}\right)=$$

$$=-\frac{1}{r}\frac{\partial P}{\partial \theta}+\mu\left\{\frac{\partial}{\partial r}\left[\frac{1}{r}\frac{\partial}{\partial r}(rU_\theta)\right]+\frac{1}{r^2}\frac{\partial^2 U_\theta}{\partial \theta^2}+\frac{2}{r^2}\frac{\partial U_r}{\partial \theta}+\frac{\partial^2 U_\theta}{\partial z^2}\right\} \tag{6}$$

z – component:

$$\rho\left(U_r\frac{\partial U_Z}{\partial r}+\frac{U_\theta}{r}\frac{\partial U_Z}{\partial \theta}+U_Z\frac{\partial U_Z}{\partial Z}\right)=-\frac{\partial P}{\partial z}+\mu\left[\frac{1}{r}\frac{\partial}{\partial r}\left(r\frac{\partial U_Z}{\partial r}\right)+\frac{1}{r^2}\frac{\partial^2 U_Z}{\partial \theta^2}+\frac{\partial^2 U_Z}{\partial z^2}\right] \tag{7}$$

Mass transfer equation in cylindrical co-ordinates:

$$U_r\frac{\partial C}{\partial r}+\frac{U_\theta}{r}\frac{\partial C}{\partial \theta}+U_Z\frac{\partial C}{\partial z}=D\left[\frac{1}{r}\frac{\partial}{\partial r}\left(r\frac{\partial C}{\partial r}\right)+\frac{1}{r^2}\frac{\partial^2 C}{\partial \theta^2}+\frac{\partial^2 C}{\partial z^2}\right] \tag{8}$$

Let *q* be the mass flow rate:

$$q=\frac{\rho v\pi D_h^2}{4}\,[\mathrm{kgs^{-1}}] \tag{9}$$

The fluid density is represented by ρ, D_h is the hydraulic diameter, and the inlet velocity is denoted by *v*, as shown below:

$$v=\frac{\mathrm{Re}\,\mu}{\rho D_h}\,[\mathrm{ms^{-1}}] \tag{10}$$

The pumping power is:

$$Q_{\mathrm{pump}}=\frac{q}{\rho}\Delta p\,W \tag{11}$$

where Δp is the pressure drop. The coefficient of variation, *CoV*, is:

$$CoV=\frac{\sigma}{\overline{C}} \tag{12}$$

One can determine the mean concentration value from the examination of the sample using:

$$\bar{C} = \frac{1}{N}\sum_{i}^{N} C_N \tag{13}$$

where C_i is the punctual concentration of pixels, $\bar{C}$ – the average concentration, and N – the number of sampling points. The standard deviation of a large data set is given by:

$$\sigma = \sqrt{\frac{1}{N}\sum_{i}^{N}(C_i - \bar{C})^2} \tag{14}$$

The value of the coefficient of variation, in general, is given by:

$$CoV = \frac{\sqrt{\frac{1}{N}\sum_{i}^{N}(C_i - \bar{C})^2}}{\bar{C}} \tag{15}$$

The mixing index can be expressed:

$$MI = 1 - CoV \tag{16}$$

$$MI = 1 - \frac{\sqrt{\frac{1}{N}\sum_{i}^{N}(C_i - \bar{C})^2}}{\bar{C}} \tag{17}$$

For this, we prefer to define the index of the mixture by equation:

$$MI = 1 - \frac{\sqrt{\sigma^2}}{\sqrt{\sigma_{\max}^2}} \tag{18}$$

where σ is the standard deviation at channel outlet and $\sigma_{\max}$ – the maximum standard deviation at the channel input where the mixing is not yet performed. Another way to calculate the mixing efficiency is by:

$$MI = 1 - \frac{\sqrt{\frac{1}{N}\sum_{i}^{N}(C_i - \bar{C})^2}}{\sqrt{\frac{1}{N}\sum_{i}^{N}(C_0 - \bar{C}_0)^2}} \tag{19}$$

The mixing indexes were calculated based on:

$$MI = 1 - \frac{\int_0^H |C_i - C_\infty| \mathrm{d}y}{\int_0^H |C_0 - C_\infty| \mathrm{d}y} \tag{20}$$

where C_0 represents the unmixed pixel concentration in the unmixed section, H – the width of the section, while C_∞ refers to the total mixed concentration.

Results and discussions

The flow fields are highlighted in this section for various inlet velocities. The Reynolds number was changed from 100 to 2500. The 3-D streamlines are plotted in fig. 4 for Re = 100, 2000, and 2500, respectively. As clearly observed, the spherical shape of the static mixer and the position of inlets and outlets generate tangential flows. The flow intensity tends to increase rapidly with the rise of Reynolds number.

The streamlines are also presented across a vertical plane, fig. 5, to explain further the flow structures generated in the chamber. At a low Reynolds number (of 100), two recirculation loops are formed in the upper and lower part of the sphere. However, four recirculation loops are generated with increased Reynolds number (at Re = 1000).

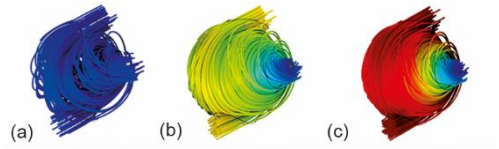

Figure 4. Streamlines for different inlet velocities; (a) Re = 100, (b) Re = 2000, and (c) Re = 2500

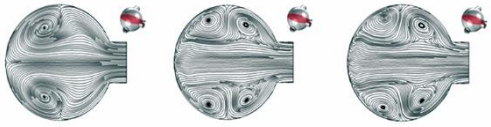

Figure 5. Distribution of the flow fields on the vertical plane; (a) Re = 100, (b) Re = 2000, and (c) Re = 2500

These toroidal vortices result from the wall effect, which intensifies the tangential motion of the fluid. At a low Reynolds number, the motionless mixers divide and redistribute the flows sequentially by utilizing only the fluid flow energy.

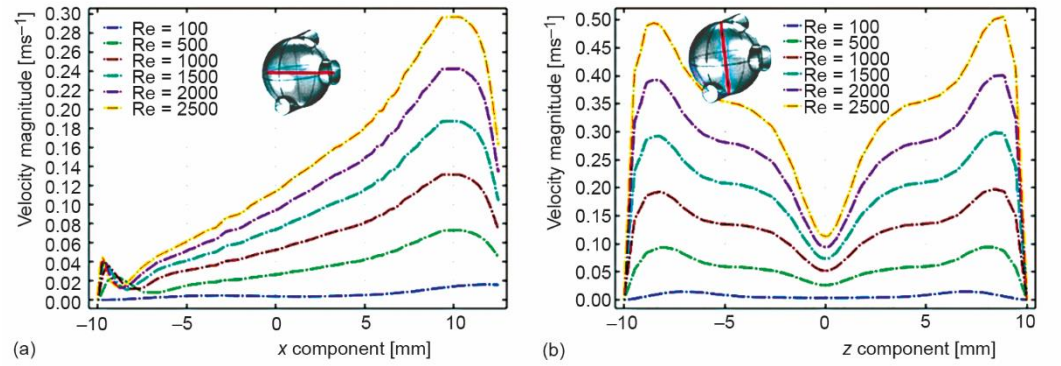

Figure 6. Velocity along; (a) *X*- and (b) *Z*-axes

Further details on the particle velocity are provided in fig. 6, where the velocity curves are plotted at various locations in the sphere. The concentration fields are illustrated in this section for various inlet velocities, fig. 7. When the Reynolds number is low (Re = 100), there is not enough agitation at the mixer center, where two cores of the fluid with different concentrations are located. However, the sufficient increaser of Reynolds number yields intensified interaction between the fluid particle, which generates a homogenous area at the center and near the mixer outlet. We note that in the deep laminar conditions, the mixing is achieved only by molecular diffusion, and no convective mixing is conducted.

For further explanation of the mixing mechanism, the streamlines are plotted with the concentration fields in fig. 8, and the concentration curves are given in fig. 9 for different positions in the chamber. The prototypical design of the suggested mixer allows a fluid redistribution in the tangential and radial directions, which are transverse directions to the main flow.

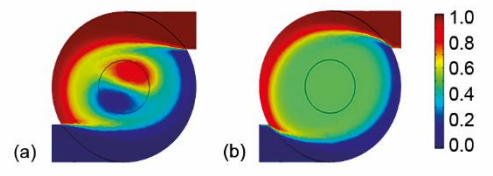

Figure 7. Distribution of the concentration; (a) Re = 100 and (b) Re = 2000

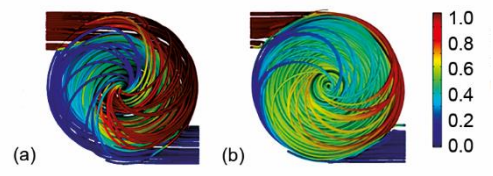

Figure 8. Concentration along streamlines; (a) Re = 100, (b) Re = 2000

The efficiency of this redistribution depends on the aspect ratio of the sphere diameter to the inlet diameter and the velocity inlet. The efficiency of the studied mixer remains in its ability to induce combined radial and tangential motions of fluid particles to bring the fluid particles into proximity, resulting thus in a fast diffusion.

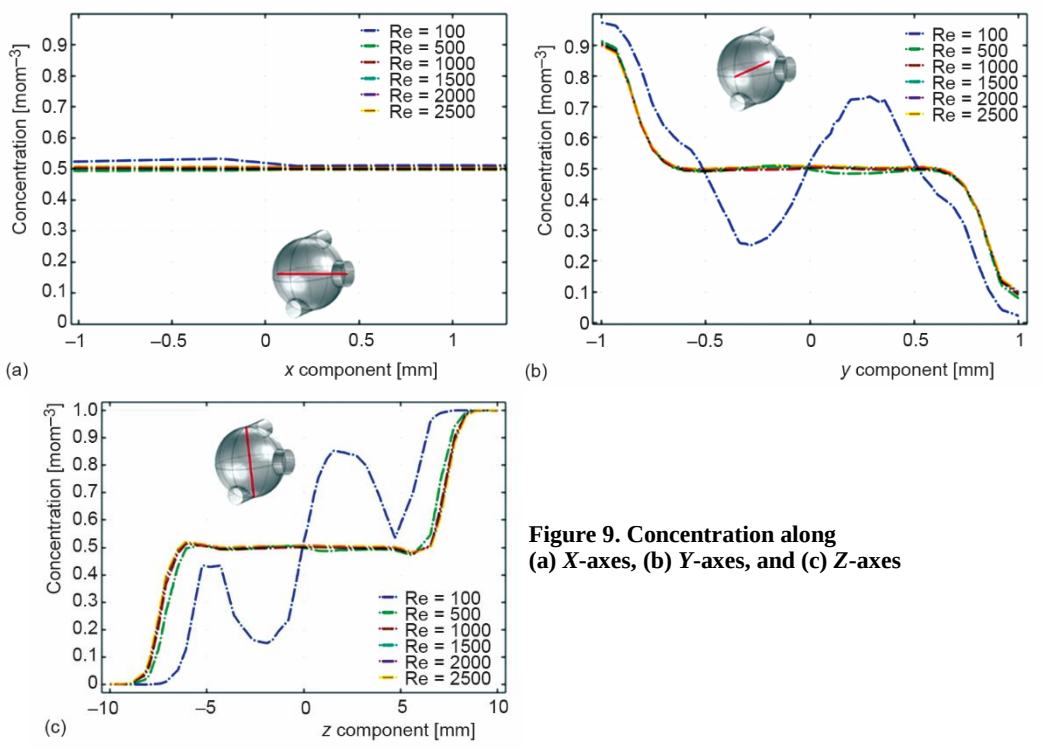

Figure 9. Concentration along (a) *X*-axes, (b) *Y*-axes, and (c) *Z*-axes

It is unnecessary to have a high-pressure drop in pipelines since the high pumping power ensures fluid-flow. It should be as low as possible to reduce wasted power during processes. An optimized level of homogeneity of mixing fluids can be achieved by selecting appropriate static mixers with the lowest pressure loss. In fig. 10, the variations of pressure drop in

the static mixer are shown for different values of Reynolds numbers (Reynold number varies from 100-2500).

As a result of these newly developed approaches, the pressure drop is lower than in existing static mixers. Thus, the new configuration of these static mixers is suitable for industries that need a simple, robust design. Additional results on the pressure distribution inside the T-mixer are provided in figs. 11 and 12 for different flow conditions and various locations in the mixer.

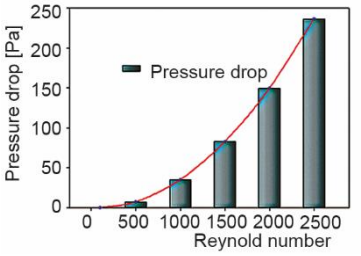

Figure 10. Pressure drop across the mixer

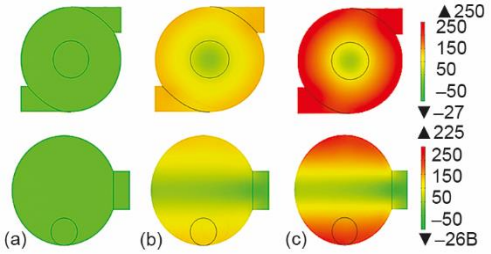

Figure 11. Pressure drop; (a) Re = 100, (b) Re = 2000, and (c) Re = 2500

The motionless mixers are utilized in multiple applications, including liquid, gas, liquid, solid, and solid-solid systems. As reported by many researchers, static mixers are known for their typically low energy requirements and limited maintenance inquiries due to the absence of moving elements. They offer satisfactory homogenization rates of fluids with a minimum residence time.

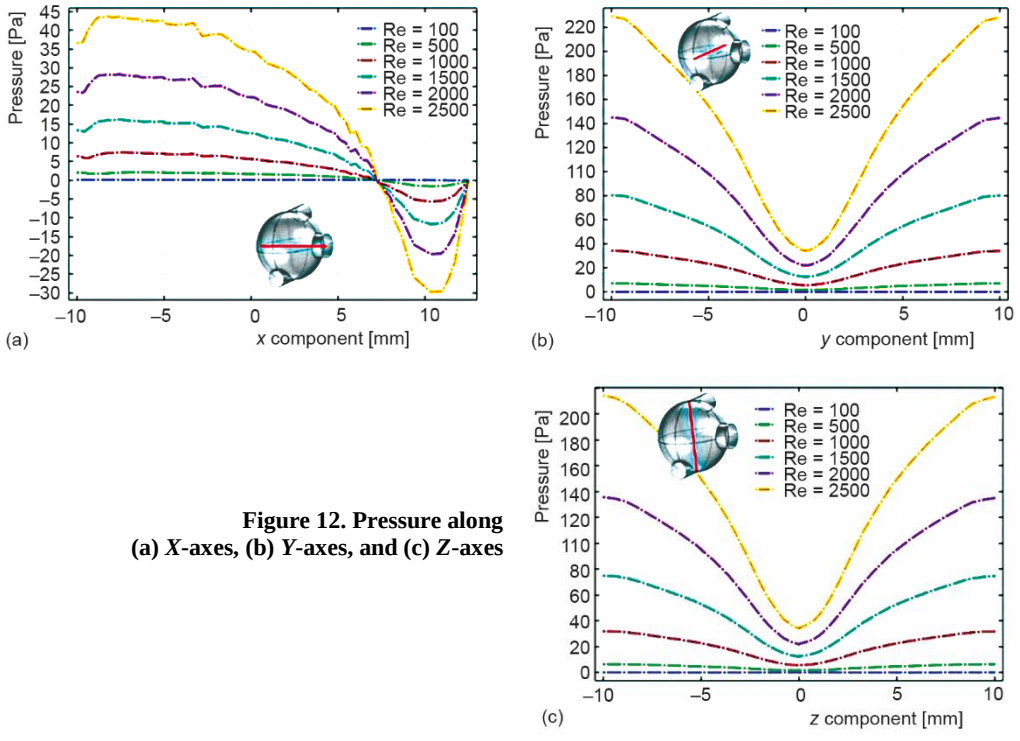

Figure 12. Pressure along (a) *X*-axes, (b) *Y*-axes, and (c) *Z*-axes

The studied static mixer ensures fluid homogenization by redistributing the fluid particles in the combined tangential and radial directions. The mixing at low levels of Reynolds numbers in undisturbed laminar conditions revealed clear spatial inhomogeneities in composition.

As confirmed by the results of the mixing index provided in fig. 13, the mixing levels increase accordingly to the rise of Reynolds number. However, the mixing index achieves its maximum at Re = 650. From Re = 750, no further enhancement of the mixing level was obtained, but only increased power pumping, fig. 14.

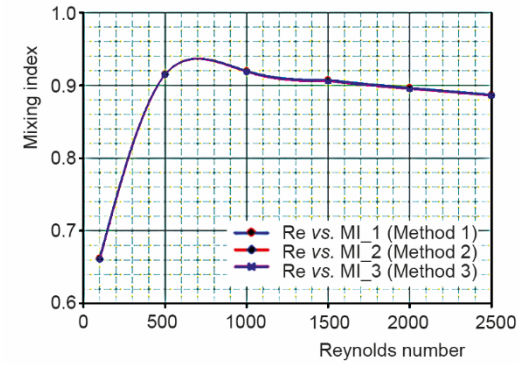

Figure 13. Mixing index

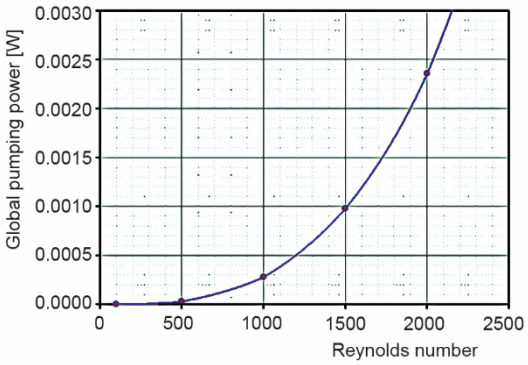

Figure 14. Pumping power

Conclusions

The performances and characteristics of a T-mixer were numerically explored. Two fluid concentrations were utilized at the inlet sections of the mixer. Flow fields, concentration fields, pressure drop, mixing index, and pumping power were determined as the main physical parameters allowing a sufficient understanding of the mixing mechanism.

- The results revealed a continuous increase in the pressure drop and pumping power with the augmented Reynolds number.
- In the deep laminar flow regime, two spatial inhomogeneities were observed.
- The highest mixing index of 0.94 reached Re = 650 and remained constant until Re = 750. However, a slight decrease in the mixing index was observed for Re > 750.
- From these findings, the best operating condition for the suggested geometrical configuration is Re, varying within 650-750.

For future studies, it is recommended to conduct further investigations to explore the effect of various parameters on the optimal design of the T-mixer. Specifically, the aspect ratio (inlet diameter to sphere diameter) should be studied to determine its impact on the mixing efficiency. The position of the inlet and outlet sections should also be analyzed to optimize their placement for maximum mixing performance. Additionally, the impact of fluid properties, such as viscosity and density, should be investigated to understand how they affect the mixing mechanism.

Acknowledgment

Researchers Supporting Project number (RSP2023R397), King Saud University, Riyadh, Saudi Arabia

References

[1] Thakur, R. K., *et al.*, Static Mixers in the Process Industries – A Review, *Chemical Engineering Research and Design*, *81* (2003), 7, pp. 787-826
[2] Hobbs, D. M., Muzzio, F. J., Reynolds Number Effects on Laminar Mixing in the Kenics Static Mixer, *Chemical Engineering Journal*, *70* (1998), 2, pp. 93-104
[3] Yoo, W. S., *et al.*, A Novel Effective Micromixer Having Horizontal and Vertical Weaving Flow Motion, *Journal of Micromechanics and Microengineering*, *22* (2012), 3, 035007
[4] Bakker, A., LaRoche, R. D., Modeling of the Turbulent Flow in HEV Static Mixers, Published in "The Online CFM Book" at http://www.bakker.org/cfm, Updated: February 15, 2000
[5] Kim, Y., *et al.*, A Novel Micro-Mixer with a Quasi-Active Rotor: Fabrication and Design Improvement, *Journal of Micromechanics and Microengineering*, *19* (2009), 10, 105028
[6] Viktorov, V., *et al.*, Numerical Study of Fluid Mixing at Different Inlet Flow-Rate Ratios in Tear-Drop and Chain Micromixers Compared to a New HC Passive Micromixer, *Engineering Applications of Computational Fluid Mechanics*, *10* (2016), 1, pp. 182-192
[7] Yang, R., *et al.*, A Rapid Micro-Mixer/Reactor Based on Arrays of Spatially Impinging Microjets, *Journal of Micromechanics and Microengineering*, *14* (2004), 10, 1345
[8] Liu, R. H., *et al.*, Passive Mixing in a Three-Dimensional Serpentine Microchannel, *Journal of microelectromechanical systems*, *9* (2000), 2, pp. 190-197
[9] Lehwald, A., *et al.*, Quantifying Macro-Mixing and Micro-Mixing in a Static Mixer Using Two-Tracer Laser-Induced Fluorescence, *Experiments in fluids*, *48* (2010), Oct., pp. 823-836
[10] Alberini, F., *Blending of Non-Newtonian Fluids in Static Mixers: Assessment via Optical Methods*, Ph. D. thesis, University of Birmingham, Birmigham, UK, 2014
[11] Fradette, L., *et al.*, Gas/Liquid Dispersions with a SMX Static Mixer in the Laminar Regime, *Chemical Engineering Science*, *61* (2006), 11, pp. 3506-3518
[12] Jegatheeswaran, S., *et al.*, Efficient Mixing of Yield-Pseudoplastic Fluids at Low Reynolds Numbers in the Chaotic SMX Static Mixer, *Chemical Engineering Journal*, *317* (2017), June, pp. 215-231
[13] Park, T., *et al.*, Effect of Static Mixer Geometry on Flow Mixing and Pressure Drop in Marine SCR Applications, *International Journal of Naval Architecture and Ocean Engineering*, *6* (2014), 1, pp. 27-38
[14] Zidouni, F., *et al.*, Simulation of Gas-Liquid Flow in a Helical Static Mixer, *Chemical Engineering Science*, *137* (2015), Dec., pp. 476-486
[15] Mihailova, O., *et al.*, Laminar Mixing in a SMX Static Mixer Evaluated by Positron Emission Particle Tracking (PEPT) and Magnetic Resonance Imaging (MRI), *Chemical Engineering Science*, *137* (2015), Dec., pp. 1014-1023
[16] Edwards, M. F., *et al.*, Mixing of Liquids in Stirred Tanks, in: *Mixing in the Process Industries*, Butterworth-Heinemann, Oxford, UK, 1992, pp. 137-158
[17] Tauscher, W., Static Mixing and Reaction Technology, *Chemical and petroleum engineering*, *32* (1996) 3, pp. 224-237
[18] Jones, D. A., Wilkinson, W. L., The Dynamic Response of a Multiple-Mixer Solvent Extraction Column to Concentration Disturbances, *Chemical Engineering Science*, *28* (1973), 2, pp. 539-551
[19] Hamouda, R. B. *Notions de Mécanique des Fluides: Cours et Exercices Corrigés*, UVT, Tunis, Tunisia, 2009
[20] Thomas, K. M., *et al.*, Design and Characterization of Kenics Static Mixer Crystallizers, *Chemical Engineering Research and Design*, *179* (2022), Mar., pp. 549-563

Paper submitted: December 18, 2022
Paper revised: Febuary 28, 2023
Paper accepted: April 14, 2023